

# Applications of cryofacies approach to frozen ground engineering – Case study of a road test site along the Alaska Highway (Beaver Creek, Yukon, Canada)



Eva Stephani<sup>1,2,3</sup>, Daniel Fortier<sup>1,3,4</sup> and Yuri Shur<sup>1,2</sup>

<sup>1</sup>*Institute of Northern Engineering, University of Alaska Fairbanks, Alaska, USA.*

<sup>2</sup>*Department of Civil and Environmental Engineering, University of Alaska Fairbanks, Alaska, USA.*

<sup>3</sup>*Center for Northern Studies, Quebec, Quebec, Canada.*

<sup>4</sup>*Department of Geography, University of Montreal, Montreal, Quebec, Canada.*

## ABSTRACT

In 2008, a test site at Beaver Creek (Yukon) was implemented to test mitigation techniques for controlling permafrost degradation along the Alaska Highway. The cryostratigraphy and soil geotechnical properties were determined based on the identification of cryofacies. The spatial distribution and typical properties of types of permafrost can be evaluated by analysis of the cryostratigraphy of permafrost cores retrieved from specific terrain units. This methodological approach allows extrapolation of the properties of frozen and thawing soils over vast areas. We present an application of the cryofacies approach to permafrost engineering, tested at the Beaver Creek experimental site.

## RÉSUMÉ

En 2008, un site expérimental visant à évaluer l'efficacité de techniques de contrôle de la dégradation du pergélisol sous l'autoroute d'Alaska a été construit à Beaver Creek (Yukon). La cryostratigraphie a été déterminée à partir de la description des cryofaciès. Les propriétés géotechniques des cryofaciès ont été mesurées en laboratoire. L'analyse des cryofaciès propres aux unités de terrain permet d'évaluer la distribution spatiale des types de pergélisol et ainsi estimer les propriétés du pergélisol sur de vastes étendues. Nous présentons ici la méthode des cryofaciès appliquée en ingénierie au cas du site expérimental de Beaver Creek.

## 1 INTRODUCTION

A significant part of the Alaska Highway is built on ice-rich permafrost. Disturbances to the natural ground during and after construction have altered the thermal regime of the permafrost and caused ground ice melting. Settlement of thawing soil has resulted in continuous road damage that is only temporarily repaired by annual maintenance operations. Taking into account high annual maintenance costs and the expected exacerbation of permafrost degradation with climate change, the Yukon Highways and Public Works (YHPW) Division is developing measures to control permafrost degradation along this widely used transportation link (Remchein et al. 2009). In 2008, the YHPW in collaboration with the Alaska University Transportation Center, University of Montreal, and Laval University established an experimental road site at Beaver Creek (Yukon) to evaluate the efficiency of 11 mitigation techniques to control permafrost degradation.

Permafrost conditions under roads must be known prior to evaluating the efficiency of mitigation measures, and to avoid costly and overly conservative measures. In a warming climate, the understanding of ground ice distribution in permafrost has important engineering and economic implications. At the Beaver Creek experimental site, detailed permafrost studies were conducted prior to design and implementation of the mitigation techniques in

order to conduct adequate monitoring of the engineering techniques being tested.

In North America, permafrost engineers and permafrost scientists have been using different methods to describe and characterize permafrost. Engineers have developed exhaustive and comprehensive procedures to determine the geotechnical properties of soils, while permafrost scientists have used geological and geomorphological techniques to understand permafrost terrain dynamics and predict spatial patterns of permafrost characteristics.

Permafrost degradation and related damage to infrastructure illustrate the urgent need to combine both expertises and develop a revised method of permafrost investigation for engineering uses. Hence, the cryofacies method (Murton and French 1994) applied to permafrost engineering aims to combine methodological strengths of permafrost science and permafrost engineering. The objective of this paper is to present the application of this method using results from the Beaver Creek experimental road site.

## 2 GROUND ICE DESCRIPTION

In North America, a simple field description of permafrost for engineering purposes has been developed by Pihlainen and Johnston (1963). According to this guide, ice is described as "not visible", "visible <1 inch thick,"

and “visible >1 inch thick,” and these three categories are subdivided. Linell and Kaplar (1966) adapted a method of description and classification of frozen soils developed by Pihlainen and Johnston (1963). In 2007, a standard procedure (ASTM D4083) was developed based on the Linell and Kaplar (1966) classification. These ground ice classifications are widely used by engineers in North America. They are simple and easy to use.

In Russia, scientists and engineers have been describing the ground ice in permafrost in terms of cryostructure types (referred to as cryotexture in Russian) and massive ice. Cryostructures are defined in terms of geometry and distribution of ice in the sediment matrix that is visible with the naked eye (Shur and Jorgenson 1998), while massive tabular ice represents large ice bodies at least 30 cm thick (Vtyurin 1975). Ground ice classifications developed by the Russians are complex and sometimes apply to permafrost containing little excess ice (Murton and French 1994). In 1994, Murton and French, inspired by Russian work, developed a cryostructure classification based on field cryofacies observed in the Western Canadian Arctic. In general, ground ice classifications need to be adapted to particular permafrost site-specific conditions.

### 3 STUDY AREA

Permafrost at the experimental site of Beaver Creek (62°20'N, 140°50'W) near the Alaskan border in the Yukon (Canada) is warm and discontinuous (Figure 1).

The continental climate in the Beaver Creek area is typified by temperature extremes in winter and summer seasons, and low annual precipitation (Scudder 1997, Rampton 1971). The mean annual air temperature (1971–2000) measured at the Beaver Creek climatic station is -5.5°C (Environment Canada 2009). The mean annual range of temperature (1971–2000) is 36.8°C. Average temperature is 12.4°C during summer (June, July, August) and -24.4°C during winter (December, January, February) (Environment Canada 2009). Thawing and freezing indexes represent an average of 1532.6 thawing degree-days and 3534.2 freezing degree-days, (1971–2000) (Environment Canada 2009). Mean (1971–2000) annual precipitation at Beaver Creek is 416.3 mm (Environment Canada 2009).

The Beaver Creek experimental site is located in an abandoned floodplain now colonized by muskeg vegetation. The silty floodplain deposits cover lodgement till (Stephani et al. 2008). No permafrost landforms such as thermokarst lakes, thermokarst pits, sinkholes, collapsed bogs, and palsa were observed in natural conditions at the experimental site.

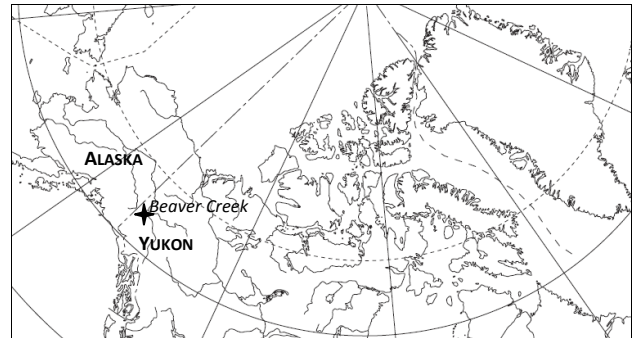


Figure 1. Location map of the Beaver Creek Experimental site in the Yukon, Canada.

### 4 METHODOLOGICAL APPROACH FOR PERMAFROST CHARACTERIZATION

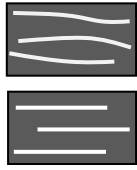
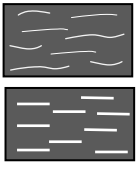
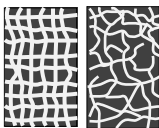
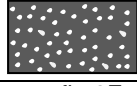
Groups of cryostructures form cryofacies, and cryofacies assemblages determine cryostratigraphic units. The cryofacies method applied to permafrost engineering should include two main components: 1) the cryostratigraphy, and 2) the geotechnical properties per cryofacies and cryostratigraphic unit.

Drilling and coring operations were conducted in August 2007, prior to construction of the experimental site. Drilling with a hydraulic rig produced continuous coring. All permafrost cores (10 cm diameters) were transported in a preserved frozen state and tested at the University of Alaska Fairbanks (UAF) geotechnical laboratory.

#### 4.1 Permafrost cores description

Prior to description, frozen cores were cleaned of the thin surficial layer of refrozen drill mud. The cores were photographed and described in terms of assemblage of sediment and cryostructure types (cryofacies). Table 1, which presents the cryostructure classification that was developed and used for description of the Beaver Creek permafrost cores, was inspired by the Murton and French (1994) classification and adapted to ground ice types observed at the Beaver Creek test site. Description of frozen soil included the shape, thickness, length, and inclination of ice inclusions, presence of air bubbles in ice, and development of the cryostructure (poorly developed to well developed). Massive ice was identified and characterized by color, dimension, and presence of air-bubbles and trace of sediments. Description of the permafrost cores also included presence of organic matter, wood fragments, and volcanic ashes (tephra). The primary sedimentary structures were described. Tables 1 and 2 list cryostructure and massive ice classifications, examples of which are shown in Figures 2 and 3.

Table 1. Cryostructure classification (inspired by Murton and French 1994).

Cryostructure name	Equivalent in other classifications	Description	Sediment type	Illustration (modified from Murton and French 1994)
Lenticular	Lenticular <sup>1</sup>	<ul style="list-style-type: none"> <li>• Lens-shaped ice in sediment;</li> <li>• Generally continuously shaped;</li> <li>• Generally horizontal (parallel to freezing front);</li> <li>• May be straight, wavy, inclined, interlaced;</li> <li>• May contains ice bubbles;</li> <li>• Thickness: <math>\geq 1</math> mm</li> </ul> <p><i>Syngenetic permafrost:</i> mm to cm thick <i>Epigenetic permafrost:</i> cm to dm thick</p> <ul style="list-style-type: none"> <li>• Usually ice-rich sediment.</li> </ul>	<ul style="list-style-type: none"> <li>• Silt to fine sand</li> <li>• Silty clay</li> </ul>	<p>see fig.3A</p> 
Microlenticular	Lenticular <sup>1,2</sup>	<ul style="list-style-type: none"> <li>• Lens-shaped ice in sediment;</li> <li>• Generally discontinuously shaped;</li> <li>• Generally horizontal (parallel to freezing front);</li> <li>• May be straight, wavy, inclined, interlaced;</li> <li>• Very few ice bubbles;</li> <li>• Thickness: <math>&lt; 1</math> mm;</li> <li>• Usually ice-rich sediment:</li> </ul> <p><i>Syngenetic permafrost:</i> <math>&gt; 50\%</math> volume <i>Epigenetic permafrost:</i> 30-50% volume</p>	<ul style="list-style-type: none"> <li>• Silt to fine sand</li> <li>• Peat</li> </ul>	<p>see fig.3A</p> 
Layered/ belt-like structure	Layered <sup>1</sup>	<ul style="list-style-type: none"> <li>• Assemblage of lenticular cryostructures;</li> <li>• Thickness: centimeter to decimeter;</li> <li>• Usually ice-rich sediment.</li> </ul>	<ul style="list-style-type: none"> <li>• Silt to fine sand</li> <li>• Peat</li> </ul>	<p>see fig.3C</p> 
Ice veins		<ul style="list-style-type: none"> <li>• Ice-filled crack or fissure in sediment;</li> <li>• Thickness variable (millimeter to centimeter)</li> </ul> <p><i>Frost crack:</i> 1-5 mm thick <i>Dilation/extension cracks:</i> cm-dm thick</p>	<ul style="list-style-type: none"> <li>• All types</li> </ul>	
Reticulate	Reticulate <sup>1,2</sup>	<ul style="list-style-type: none"> <li>• Net-like cryostructure of interconnected sub-horizontal ice lenses and sub-vertical ice veins;</li> <li>• Usually ice-rich to very ice-rich sediment (<math>\approx 35-95\%</math> volume).</li> </ul>	<ul style="list-style-type: none"> <li>• Silt to fine sand</li> </ul>	<p>see fig.3F</p> 
Suspended	Suspended <sup>1</sup> ; Ataxitic <sup>2</sup>	<ul style="list-style-type: none"> <li>• Suspended aggregates in ice;</li> <li>• Usually very ice-rich sediment (up to 90-95% volume);</li> <li>• Common in upper part of permafrost</li> </ul>	<ul style="list-style-type: none"> <li>• Silt to fine sand</li> <li>• Occasionally peat</li> <li>• Silty clay</li> </ul>	<p>see fig.3E</p> 
Crustal	Crustal <sup>1,2</sup>	<ul style="list-style-type: none"> <li>• Ice-coating around rock fragments, aggregates or wood fragments;</li> <li>• Usually partial coating, occasionally total;</li> <li>• Common just beneath permafrost table;</li> <li>• Thickness: few millimeters to centimeter thick coating.</li> </ul>	<ul style="list-style-type: none"> <li>• Gravel/rock fragments</li> <li>• Diamicton</li> </ul>	<p>see fig.3D</p> 
Porous visible	Ice cement <sup>1</sup> ; Massive <sup>2</sup>	<ul style="list-style-type: none"> <li>• Pore ice that is visible to the unaided eye;</li> <li>• Usually ice-poor sediment (<math>&lt; 30\%</math> volume).</li> </ul>	<ul style="list-style-type: none"> <li>• Gravel/rock fragments</li> <li>• Diamicton</li> </ul>	<p>see fig.3F</p> 
Porous invisible	Ice cement <sup>1</sup> ; Massive <sup>2</sup>	<ul style="list-style-type: none"> <li>• Pore ice not visible to the unaided eye;</li> <li>• Usually very ice-poor sediment (<math>&lt; 10-30\%</math> volume).</li> </ul>	<ul style="list-style-type: none"> <li>• All types</li> </ul>	<p>see fig.3F</p> 

<sup>1</sup> Murton and French (1994); <sup>2</sup> Kudriavtsev (1979)

Legend: Grey = sediment; Dark grey = aggregates or wood fragments; White = ice.

Table 2. Type of massive ice observed at Beaver Creek.

<p><b>Wedge ice:</b> (Figure 2 and 3G):</p> <ul style="list-style-type: none"> <li>• Vertically foliated ice</li> <li>• Rich in large (mm) air bubbles</li> <li>• Contains sediment/organic traces vertically aligned</li> </ul>	
<p><b>Ice wedge:</b></p> <ul style="list-style-type: none"> <li>• V-shaped</li> <li>• Enclosing sediments may be uplifted at the ice wedge contact (oblique to sub-vertical contact)</li> <li>• <i>Syngenetic</i>: Tends to develop in height (chevron like)</li> </ul>	<p><i>Epigenetic</i>: Tends to develop in width</p>  

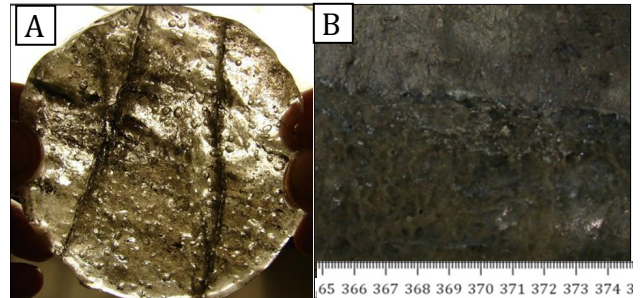


Figure 2. A) Example of wedge ice core cross-section. Two sets of ice veins are intersecting. Note the presence of air bubbles and mineral-to-organic inclusion (dark) within the ice. B) Example of wedge ice contact with enclosing sediment within a core (scale in cm).



Figure 3. Cryostructure examples. Black is ice. A) lenticular (>1 mm thick) and microlenticular (<1 mm thick); B) poorly developed reticulate; C) belt-like cryostructure; D) crustal; E) suspended; F) porous; G) wedge ice.

#### 4.2 Geotechnical properties of the permafrost soil

Laboratory soil tests were conducted on samples from each cryofacies.

Moisture content was determined by oven-drying soil at 90°C for 72 h. The gravimetric moisture content was determined for each oven-dried sample, while the volumetric ice content was measured on cores with a well-preserved cylindrical shape only.

Thaw strain ( $\delta$ ) was measured on frozen cores with a well-preserved shape. Firstly, a frozen core of known

dimensions was inserted in a transparent acrylic cylinder, where it was thawed at room temperature in undrained conditions without applied load (Figure 4). The height of the thawed core was estimated from several height measurements of the soil in the cylinder (Figure 4). Secondly, sub-samples from samples thawed without external load were placed in the consolidation apparatus to evaluate the void ratio and strain after applying incremental loads (ASTM-D2435 2004). Finally, thaw strain was evaluated as (Grechishchev and Shur 1990):

$$\delta = \delta_1 + \delta_2 - \delta_1 \delta_2 \quad [1]$$

where  $\delta$  = total thaw strain,  $\delta_1$  = thaw strain of frozen soil without external load, and  $\delta_2$  = strain of thawed soil under load.

Thaw strain can also be evaluated from soil index properties by using well-known Equation 2:

$$\delta = \frac{e_i - e_f}{1 + e_i} \quad [2]$$

where  $e_i$  = initial void ratio (Eq. 3),  $e_f$  = final void ratio, for saturated soil

$$e_i = 1.09WG_s \quad [3]$$

where  $W$  = moisture content and  $G_s$  = specific gravity (2.65 assumed if not measured for sample).

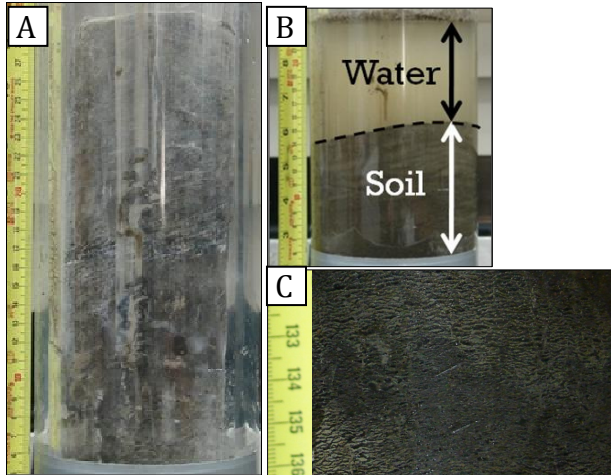


Figure 4. Thaw-strain test example. A) frozen core in thaw-strain cell; B) thawed core; C) micro-lenticular cryostructure observed in the core prior to the test (black is sub-mm ice lenses).

The American Society of Testing and Materials (ASTM) test procedures were used to determine particle-size distribution (ASTM-D422 2007), specific gravity (ASTM-D854 2006), organic content (ASTM-D2974 2007), Atterberg limits (ASTM-D4318 2000), and thermal conductivity (ASTM-D5334 2008).

The electrical conductivity and the pH were measured in thawed soil.

## RESULTS

Table 3 illustrates an example of cryofacies description with some of the geotechnical properties for a borehole in the natural ground adjacent to the road. The permafrost at Beaver Creek is presented in three cryostratigraphic units (Stephani et al. 2008). Unit 1 (0–1.0 m) is composed of ice-rich peat with some silt and volcanic ash. It represents a terrestrial fen peat environment affected by alluvial activity. Unit 2 (1.0–6.5 m) is composed of silt and is divided into three sub-units. Sub-unit 2A (<2.0 m) comprises ice-rich silt. Sub-unit 2B (2.0–3.5 m) is ice-poor silt and sub-unit 2C (3.5–6.5 m) is ice-rich silt. The top of a buried (inactive) ice-wedge network observed in the boreholes is located in ice-poor sub-unit 2B. The top of the ice-wedge network is located ~2.5 m under the surface; the ice wedges extend down at least 10 m deep.

Unit 2 is identified as a low-energy meandering alluvial plain deposit. Unit 3 (6.5–10.0 m) comprises an ice-rich diamict, partially reworked and mixed with peat in the upper portion of the unit, whereas the lower portion comprises sub-angular to rounded rock fragments in a sandy to silty matrix. Unit 3 has been interpreted as a lodgement till; the upper surface has been reworked by alluvial activity and locally colonized by muskeg vegetation.

Micro-lenticular, lenticular, layered, and suspended cryostructures were generally well developed in syngenetic permafrost (e.g., ice-rich layers of unit 2), while the porous visible and invisible cryostructures were observed in epigenetic permafrost such as in the ice-poor layer of unit 2. Suspended, lenticular, and crustal cryostructures observed within unit 3 indicate epigenetic permafrost propagation within fine-grained till.

Figures 5 to 7 show thaw strain with incremental loads for the three cryostratigraphic units, and Table 4 compiles the void ratio variations.

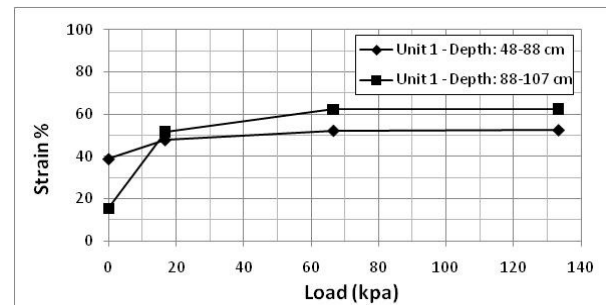


Figure 5. Thaw strain with incremental loading of samples from unit 1.

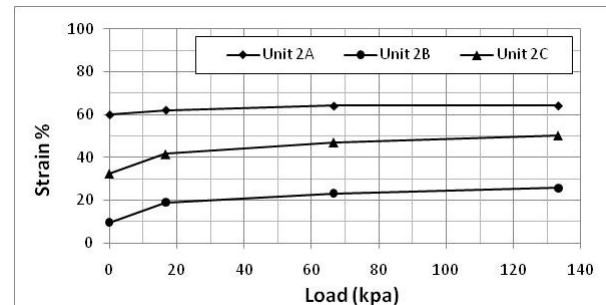


Figure 6. Thaw strain with incremental loading of samples from unit

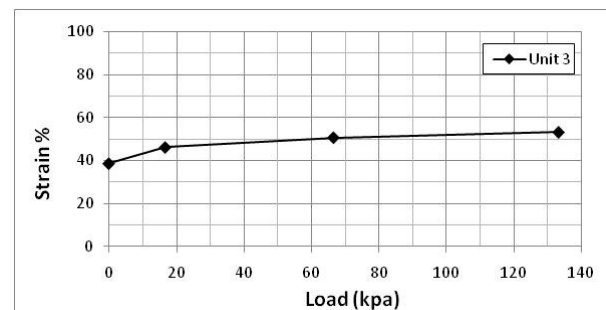


Figure 7. Thaw strain with incremental loading of a sample from unit 3 (organic rich sample).

Table 3. Cryofacies and their properties for a borehole located in the natural ground adjacent to the road.

Depth (cm)	Cryofacies description	Unit	W <sub>g</sub> (%)	OC (%)	Grain-size distribution				LL (%)	PL (%)
					Gravel (%)	Sand (%)	Silt (%)	Clay (%)		
0-48	Organic cover (thawed)	1	-	-	-	-	-	-	-	-
48-100	Reworked ice-rich peat, silt and tephra. Wood chunks at 68-77 cm. Dominant cryostructure: lenticular and reticulate.	1	160	13.7	0	28	57	15	50	34
100-190	Ice-rich peaty silt to silty peat. Dominant cryostructure: microlenticular, 10 mm thick ice lens at 140 cm.	2A	110	7.2	0	14	73	13	34	28
190-276	Ice-poor grey silt. Dominant cryostructure: porous invisible to visible, and sparse poorly developed microlenticular.	2B	32	3.3	0	10	78	12	25	23
276-360	Wedge ice	2B	-	-	-	-	-	-	-	-
360-420	Ice wedge lateral contact with silty peat. Dominant cryostructure in silty peat: microlenticular.	2B	-	-	-	-	-	-	-	-
420-630	Ice-rich peaty silt to silty peat. Dominant cryostructure: microlenticular to lenticular. Belt-like structures at 440 cm, 500-522 cm.	2C	105	9.8	1	11	78	10	46	39
630-842	Ice-rich diamicton (fine-grained matrix) with decimeters thick peatier diamicton layers increasing with depth. Dominant cryostructure: porous visible, lenticular and suspended.	3	85	7.5	20	26	44	10	27	25
842-1009	Alternate ice-rich decimeter thick layers of woody brown peat, woody slightly stratified grey silt, and diamicton. White tephra layer at 989-993 cm. Dominant cryostructure: Poorly developed microlenticular in silt, porous invisible to visible in peat, lenticular to suspended in the vicinity of larger wood fragments, and lenticular and porous visible in diamicton. Ice vein connecting from 891 cm to underlying ice wedge.	3	39	33.6	20	56	17	7	-	-
1009+	Wedge ice	-	-	-	-	-	-	-	-	-

*Legend:* W<sub>g</sub> = Gravimetric ice content; W<sub>v</sub> = Volumetric ice content; OC = Organic matter content; LL = Liquid limit; PL = Plastic limit

Table 4. Void ratio variations with incremental loading per cryostratigraphic unit.

Load (KPa)	Void ratio					
	Unit 1	Unit 1	Unit 2A	Unit 2B	Unit 2C	Unit 3
0 (frozen)	4.48	4.62	4.20	1.04	3.59	4.34
0 (thawed)	3.63	2.43	1.08	0.85	2.10	2.28
16.7	1.65	1.93	0.97	0.65	1.68	1.88
66.6	1.07	1.68	0.87	0.57	1.43	1.64
133.3	1.05	1.67	0.86	0.52	1.28	1.51

## DISCUSSION

Cryostructures are related to soil type and the freezing process of the ground during permafrost aggradation.

Layered, lenticular, and microlenticular cryostructures are the result of ice segregation in the sediment. These

cryostructures are typical of fine-grained syngenetic permafrost. Thick ice lenses spaced by soil with low water content tend to develop in epigenetic permafrost, especially at depth.

Suspended cryostructures are typical of the very ice-rich intermediate layer (Shur 1988) and represent the formation of aggradational ice in association with aggradation of permafrost in the previously thicker active layer.

Porous visible and invisible cryostructures result from in-freezing of water trapped in the soil pores without additional water movement to the freezing soil. These cryostructures prevail in coarse-grained sediments. These relatively ice-poor cryofacies can also be developed in fine-grained sediments that were originally ice-rich, thawed, drained, and refrozen (Shur and Zhestkova, 2003). The ice-poor silt of sub-unit 2B at Beaver Creek experienced these processes.

The assemblage of ice veins and ice lenses in a net-like structure forms the reticulate cryostructure that can be formed in epigenetic and syngenetic permafrost conditions.

The contiguous assemblage of ice veins results in the formation of ice wedges (massive ice) that are distributed as networks of ice-wedge polygons. Ice wedge size varies according to permafrost and sediment types. In syngenetic permafrost, the height and width of the ice wedges are a function of the sedimentation rate. The ice wedges in syngenetic permafrost follow upward the rising surface during sedimentation. Very large ice wedges can develop in colluvial and eolian deposits over thousands of years in sediments known as yedoma (ice complex) (Baulin and Murzaeva, 2003). Epigenetic ice wedges are formed after aggradation of the permafrost after sediment deposition. They essentially develop in width, not depth (Mackay 1990).

Identification of cryofacies, with their typical cryostructures, and knowledge of their characteristic properties allow rapid evaluation of the excess ice content of the frozen ground in the terrain of interest.

Micro-lenticular, lenticular, layered, reticulate, and suspended cryostructures that are well developed indicate that the soil is ice-rich to very ice-rich. At the Beaver Creek experimental site, cryofacies comprising such cryostructures had gravimetric moisture content between 105% and 160% (Table 3). Permafrost with these cryostructures at Beaver Creek has significant thaw strain ( $\geq 0.4$ ). Ice in soils with well-developed micro-lenticular cryostructure ( $< 1$  mm thick) is hardly visible, and soil could be misinterpreted as having "no visible ice," according to some ground ice classifications (Pihlainen and Johnston 1963, Linell and Kaplar 1966, ASTM 2007), and thus could be considered ice-poor, which would underestimate the significant thaw strain typical to that soil.

Porous visible and invisible cryostructures, crustal cryostructure, and isolated ice veins characterize ice-poor sediments in comparison with soils having a lenticular cryostructure. At Beaver Creek, sub-unit 2B with grey silt and porous (invisible to visible) cryostructure had an average gravimetric ice content of 32% (Table 3). Soil will not experience thaw settlement that is hazardous to roads, because excess ice content is low or inexistent. However, if drainage of this thawing layer is impeded, soil could have high liquefaction potential since it becomes saturated after thawing (Table 3).

Due to their spatial distribution, ice wedges were not encountered in some boreholes and were not found at the same depth when the side of a wedge was cored through. Ice-wedge polygons, and especially syngenetic ice wedges, are complex. They do not always have surface manifestation, and their patterns are difficult to predict. At Beaver Creek, the buried network of ice wedges does not have obvious surface expression, which stresses the importance of identifying the type of massive ice encountered in boreholes. Misinterpretation of the potential distribution of ice wedges frequently results in significant engineering miscalculations.

Applications of cryofacies analysis for engineering purposes include efficient evaluation of thaw susceptibility of soils under the road, which is of great concern for the preservation of road integrity.

The Beaver Creek experimental site has been built on unit 1 strata (ice-rich peat mixed with some silt and

volcanic ash) that are thawing in several locations. Evaluation of thaw strain of this soil (Table 4 and Figure 5) shows that thawing of upper permafrost with high excess-ice content results in great thaw settlement. Sub-unit 2A (ice-rich silt) underlies unit 1 along the entire test site. The variable distribution of ice-rich cryofacies within this sub-unit results in differential thaw settlement when the permafrost thaws (Table 4 and Figure 6). The silt that composes unit 2 and its three sub-units prevents rapid drainage of thawed soils. The underlying ice-poor soil of sub-unit 2B is thaw-stable ( $\delta \leq 0.1$ ) between ice wedges (Figure 6). However, thawing of ice wedges within this sub-unit will create sinkholes and large depressions. In some cases, groundwater flow can trigger rapid linear erosion of the ice wedges (Fortier et al. 2007), which can result in highly differential thaw settlement of sub-unit 2B, where wedge ice melts and ice-poor silt remains stable. The low hydraulic conductivity of silt does not favour groundwater flow in sub-unit 2B except locally at the interface with sandier horizons (higher hydraulic conductivity). Ice wedges penetrate the underlying sub-unit. Deep ice-wedge degradation can therefore trigger permafrost degradation in the sediment adjacent to the ice wedges. Due to the great depth of ice wedges, their degradation and associated issues may not be encountered until well into the later stages of permafrost degradation. Sub-unit 2C, which is similar to sub-unit 2A, is also highly thaw-susceptible (Figure 6) and is characterized by differential thaw settlement potential due to the variable distribution of its cryostructures (and ground ice content).

The upper part of unit 3 is ice-rich but with variable ice content due to reworking of the diamicton and presence of peat layers. Thawing of unit 3 will require considerable extraction of latent heat because of the high ice content of the diamicton. Once this is done, melting of ground ice will result in significant thaw strain (Table 4 and Figure 7).

## CONCLUSION

The cryofacies method requires identification of typical cryostructures that are characterized by a range of geotechnical properties. The method enables extrapolation of frozen ground properties, thaw sensitivity, and the processes triggered by degradation (e.g., differential thaw settlement, linear erosion) over vast areas after evaluation for typical cryofacies. Statistical relationships between cryofacies and soil geotechnical properties can also be established.

Cryofacies at the Beaver Creek experimental site, located in warm discontinuous permafrost, are highly susceptible to thermal degradation and to differential thaw settlement. Three ice-rich cryostratigraphic units have been identified, of which only one sub-unit is ice-poor. However, this ice-poor sub-unit comprises buried ice wedges. Thus, permafrost at Beaver Creek experimental site has been determined as thaw-susceptible.

The cryofacies method used to describe permafrost conditions at Beaver Creek is efficient in estimating permafrost properties within extensive areas that correspond to the same terrain units (e.g., alluvial plain,

lodgement till, drained lake). This approach enables the evaluation of potential processes of permafrost degradation related to cryostratigraphy and local terrain conditions, as well as the prediction of permafrost properties and behaviour in frozen and thawing states. The cryofacies method helps obtain a dynamic assessment of permafrost conditions for engineering applications.

#### ACKNOWLEDGMENTS

This work has been supported by the Alaska University Transportation Center, the UAF Institute of Northern Engineering, and Yukon Highways and Public Works. The first author is a postgraduate fellow of the National Sciences and Engineering Research Council of Canada.

Special thanks to Michel Sliger, Rachel Thériault, and Kouli Kim, students who contributed to the soil laboratory testing. The authors also acknowledge valuable discussions with Mikhail Kanevskiy and the paper review by Steve Kokelj and Fran Pederson.

Opinions expressed are those of the authors and do not necessarily reflect those of the funding institutions.

#### REFERENCES

- ASTM Standard D5334, 2008. *Determination of the thermal conductivity of soil and soft rock by thermal needle probe procedure*, ASTM International, PA, USA.
- ASTM Standard D422, 2007. *Particle-size analysis of soils*, ASTM International, PA, USA.
- ASTM Standard D2974, 2007. *Moisture, ash, and organic matter of peat and other organic soils*, ASTM International, PA, USA.
- ASTM Standard D4083, 2007. *Description of frozen soils (visual-manual procedure)*, ASTM International, PA, USA.
- ASTM Standard D854, 2006. *Specific gravity of soil solids by water pycnometer*, ASTM International, USA.
- ASTM Standard D2435, 2004. *One-dimensional consolidation properties of soils using incremental loading*, ASTM International, PA, USA.
- ASTM Standard D4318, 2000. *Liquid limit, plastic limit, and plasticity index of soils*, ASTM International, PA, USA.
- Baulin, V.V. and Murzaeva, V.E. (eds.) 2003. *Geocryological glossary*, Geos, Moscow, Russia. (In Russian)
- Environment Canada. 2009. Canadian climate normals 1971–2000, <http://www.climat.meteo.gc.ca>.
- Fortier, D., Allard, M. and Shur, Y. 2007. Observation of rapid drainage system development by thermal erosion of ice wedges on Bylot Island, Canadian Arctic Archipelago, *Permafrost and Periglac. Process.*, 18: 229-243.
- French, H.M. 2007. *The periglacial environment*, 3<sup>rd</sup> ed., John Wiley & Sons publication, London, England.
- Grechishchev, S.E. and Shur Y.L. (eds.) 1990. *Integration of composition and structure of frozen soils in evaluation of permafrost related processes (guidelines)*. Institute of hydrogeology and engineering geology, Moscow, Russia.
- Linell, K.A. and Kaplar, C.W. 1966. Description and classification of frozen soils. *1st International Conference on Permafrost*, National Academy of Science – National Research Council of Canada Publication 1287, 481-487.
- Mackay, J.R. 1990. Some observations on the growth and deformation of epigenetic, syngenetic and anti-syngenetic ice-wedges, *Permafrost and Periglac.Process.*, 1: 15-29.
- Kudriavtsev, V.A. (ed) 1979. *Methodology of permafrost survey*, Moscow State University, Russia.
- Murton, J.B. and French, H.M. 1994. Cryostructures in permafrost, Tuktoyaktuk coastlands, western Arctic, Canada. *Canadian J. of Earth Sciences*, 31: 737-747.
- Pihlainen, J.A. and Johnston, G.H. 1963. *Guide to a field description of permafrost for engineering purposes*. National Research Council of Canada, Associate Committee on Soil and Snow Mechanics, technical memorandum 79.
- Rampton, V. N. 1971. *Late Quaternary vegetational and climatic history of the Snag-Klutlan area, Southwestern Yukon Territory, Canada*, Ph.D. dissertation, Minnesota Univ., Minneapolis, USA.
- Remchein, D., Fortier, D., Dore, G., Stanley, B., and Walsh, R. 2009. Cost and constructability of permafrost test sections along the Alaska Highway, Yukon. *Transport Association of Canada Annual Conference*, Vancouver, Canada.
- Scudder, G.G.E. 1997. Environment of Yukon, *In: Insect of the Yukon. Biological Survey of Canada (Terrestrial Arthropods)*, Ottawa, 13-57.
- Shur, Y., 1988. The upper horizon of permafrost soil, *5th International Conference on Permafrost*, Trondheim, Norway, 1988, 867-871.
- Shur, Y. and Jorgenson, M.T. 1998. Cryostructure development on the floodplain of Colville River Delta, Northern Alaska, *7th International Conference on Permafrost*, Yellowknife, N.W.T., Canada, 993-999.
- Shur, Y. and Zhestkova T. 2003. Cryogenic structure of glacio-lacustrine deposit. *8th International Conference on Permafrost*, Zürich, Switzerland, Bulkeema Publishers, 1051-1057.
- Stephani, E., Fortier, D., Doré, G., Stanley, B., and Shur, Y. 2008. Preservation of the Alaska Highway, *9<sup>th</sup> International Conference on Permafrost*, Fairbanks, Alaska.
- Vtyurin, B.I. 1975. *Ground ice in the USSR*, Nauka, Moscow, Russia. (In Russian)